

16-Molecular Structure Determination by Methods other than Diffraction

Fig. 1. X-ray absorption spectrum near the Ta-L_{III} edge of KTaO₃ at 32 K.

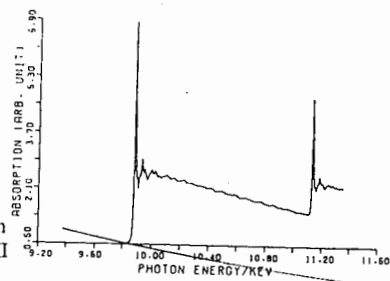
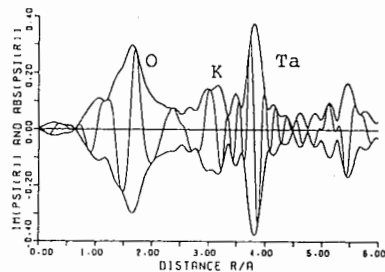


Fig. 2. Radial structure function around Ta atom at 32 K.



Harada, J., Axe, J. D. & Shirane, G. (1970). *Acta Cryst.* A26, 608.
Maeda, H. (1987). *J. Phys. Soc. Jpn.* 56, 2777.
Samara, G. A. & Morosin, B. (1973). *Phys. Rev.* B8, 1256.
Vogt, H. & Uwe, H. (1984). *Phys. Rev.* B29, 1030.

PS-16.01.07 RELATIONSHIP BETWEEN CATALYTIC ACTIVITY FOR WATER-GAS SHIFT AND STRUCTURE OF Co-Mo-Mg/Al₂O₃ CATALYST
Li Xiaoding*, Lu Xiaowan, Li Yaohui, Chen Jingsong, Kong Yuhua
Hubei Research Institute of Chemistry, Wuhan, 430074, China,

The deactivation of two commercial Co-Mo-Mg/Al₂O₃ WGS catalysts has been studied by XRD, ICP, IR, SEM, XPS etc. The results showed that formation sulfates, impurities, regenerative conditions and mechanical strength of catalyst have significant effect on the activity except ratio of steam/gas, H₂S content and operating temperature.

The Co-Mo-Mg/Al₂O₃ catalyst was prepared by incipient wetness impregnation on a γ-Al₂O₃ with a Mg(NO₃)₂ and calcined at 900°C for 2h after drying. Then this same material was impregnated with a Co(NO₃)₂ and (NH₄)₆Mo₇O₂₄ mixed solution.

A typical γ-Al₂O₃ XRD pattern was given by Co-Mo-Mg/γ-Al₂O₃ catalyst A in the oxidic state (P. J. Gajardo, *Less-Common Met.*, 1977, 54, 311). This implied that cobalt and molybdenum as well as magnesium had been well dispersed on the support. Catalyst B showed three XRD patterns consistent with MgO, Al₂O₃ and MgAl₂O₄. The crystal phases MgO and MgAl₂O₄ in the catalysts led to a gradual drop in activity (J. P. R. Visser, *Bull. Chim. Bdg.*, 1984, 93, 813). The spinel MgAl₂O₄ structure formation was observed with increasing the calcination temperature, so it is correlated with the procedure of catalyst preparation.

The specific surface areas of oxide state catalyst (>150m²/g) decrease to about 100m²/g as the catalyst converted to sulfided state. It was about 70m²/g after the catalyst used for a year, and the catalyst mechanical strength decreased to 1/3 after regeneration, comparing with new one.

The Co, Mo and Mg in catalyst were not lost after it used for four years. The ICP results of catalyst A and B are shown in Fig. 1. There was a small part of impurity K⁺ and Na⁺ in catalyst lost. The inorganic impurities in feed gas are mainly Fe, Ca, Pb and K etc. the activity is decreased with its deposition on the surface of the catalyst and it is reconverted after regeneration.

The deactivation is mainly due to the formation of sulfates, increasing of MoS₂ and MgAl₂O₄, the active center Co-Mo-S is destroyed. over-heating in the regeneration, sulfidation and operation process enhance formation of inactive MgO, MgAl₂O₄ and crystal phase MoS₂. The higher ratio of steam/gas and the higher concentration of SO₂ etc enhance also the sulfates formation.

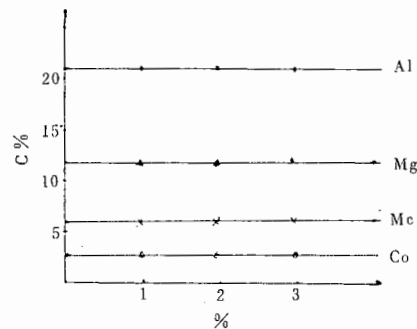


Fig. 1. ICP results of catalyst A and B.

PS-16.01.08 CRYSTAL STRUCTURE AND HALOGEN NQR OF DIAMMONIUMALKANE HALIDES. By Shi-qi Dou*, Helmut Paulus and Alarich Weiss, Institut für Physikalische Chemie, Technische Hochschule Darmstadt, Petersenstr.20, D-6100 Darmstadt, Germany.

The crystal structures of the isomorphous compounds 1,3-diammoniumpropyl- dibromide and -diiodide are reported. Monoclinic, P2₁/n, Z=4. Lattice constants in pm. (H₃N(CH₂)₃NH₃)²⁺ 2Br⁻: a= 1343.8(5), b=457.9(1), c=1347.1(5), β=109.14(1)°; (H₃N(CH₂)₃NH₃)²⁺ 2I⁻: a=1421.3(5), b=478.0(2), c=1419.6(5), β=110.10(1)°. The diammoniumpropyl cations are centrosymmetric and there are two crystallographic independent anions and two independent cations in the unit cell. The positive (H₃N(CH₂)₃NH₃)²⁺ cations and halogen anions are proportionate distributed in the lattice. Weak hydrogen bonds N-H...X-, X=Br, I are observed. The discrepancy in the ⁷⁹Br and ¹²⁷I NQR spectra, respectively, [1] from which isomorphism was denied, is removed by reinvestigation of the spectra. Additionally to the already known ⁹¹Br line at 22.95MHz a second line at 12.07MHz was found at room temperature. Structures and NQR spectra are compared and discussed.

[1]; J. Hartmann, S.-q. Dou, and Al. Weiss, *Z. Naturforsch.* 44a, 41 (1989)

PS-16.01.09 N-TRICHLORO- AND DICHLOROACETYL AMINO ACIDS AND COMPOUNDS OF AMINO ACIDS WITH HALOGENO ACETIC ACIDS. ⁵¹CL NUCLEAR QUADRUPOLE RESONANCE SPECTROSCOPY; CRYSTAL STRUCTURE OF N-TRICHLOROACETYL-GLYCINE, -DL-ALANINE, AND -L-ALANINE. By Shi-qi Dou*, Armin Kehrler, Armin R. Ofial, and Alarich Weiss, Institut für Physikalische Chemie, Technische Hochschule Darmstadt, D-6100 Darmstadt, Germany

16-Molecular Structure Determination by Methods other than
Diffraction

401

The crystal structures of N-trichloroacetyl-glycine, TCA-G, N-trichloroacetyl-DL-alanine, TCA-DL-A, N-trichloroacetyl-L-alanine, TCA-L-A have been determined. The ^{35}Cl NQR spectra of N-trichloroacetyl amino acids and dichloroacetyl-glycine, -L-alanine, and -L-valine have been measured as function of temperature. Also the compounds of glycine, L-alanine with ClF_2CCOOH , of glycine, L-leucine with ClH_2CCOOH , of glycine and L-leucine with Cl_2HCCOOH and of glycine and L-leucine with Cl_3CCOOH have been studied by ^{35}Cl NQR. The structures: TCA-G: $\text{Pna}2_1$, $Z=8$, (in pm and degree) $a=1641$, $b=1002$, $c=1018$; TCA-DL-A: $\text{C}2/c$, $Z=8$, $a=3280$, $b=556$, $c=1031$, $\beta=96.68$; TCA-L-A: $\text{P}1$, $Z=2$, $a=967$, $b=949$, $c=619$, $\alpha=74.97$, $\beta=74.20$, $\gamma=61.20$.

The ^{35}Cl NQR frequencies have been observed in the range $41 \geq \nu/\text{MHz} \geq 38$, decreasing with increasing temperature. Part of the resonances bleach out at T_b , far below room temperature, leading to informations about the crystal structures at 77K. No phase transitions were observed by DTA between 77 and 295K.

The crystal structures will be discussed in connection with the spectroscopic results and conclusions will be drawn about the structures of the compounds for which ^{35}Cl NQR only is available..

PS-16.01.10 CRYSTAL STRUCTURE REFINEMENT AND SINGLE CRYSTAL ^{81}Br ZEEMAN NQR STUDY OF $\text{KHgBr}_3 \cdot \text{H}_2\text{O}$. By Hiromitsu Terao^a, Tsutomu Okuda^a, Sachiyo Uyama, Hisao Negita^a, Shi-qi Dou^b, and Alarich Weiss^c. Faculty of Integrated Arts and Sciences, Tokushima University, Minamijosanjima-cho, Tokushima 770, Japan. ^a) Department of Chemistry, Faculty of Science, Hiroshima University, Kagamiyama, Higashihiroshima 724, Japan. ^b) Computer Center, Hiroshima University of Economics, Asaminami-ku, Hiroshima, Japan. ^c) Institut für Physikalische Chemie, Technische Hochschule Darmstadt, Petersenstr.20, D-6100 Darmstadt, Germany.

From ^{81}Br NQR Zeeman spectroscopy the electric field gradient tensors, EFGT, at the Br sites of $\text{KHgBr}_3 \cdot \text{H}_2\text{O}$ were determined in magnitude and direction of Φ_{xx} , Φ_{yy} , and Φ_{zz} . For Br(1) and Br(2) the bond directions $r(\text{Hg}-\text{Br})$ found in the structure determination [1] do not agree with the direction of Φ_{zz} we measured. Also for the bridging bromine Br(3) there is a discrepancy with the NQR results. Structure and ^{81}Br NQR are in contradiction. Therefore the crystal structure was redetermined. We find the same space group, $\text{Cmc}2_1$, $Z=4$, $a=436.5(2)\text{pm}$, $b=1689.6(5)\text{pm}$, $c=1015.0(4)\text{pm}$, nearly the same lattice constants as [1]. However the structure found differs from [1] in the atomic positions and the coordination model changes drastically. With the redetermination, ^{81}Br NQR and structure are in good agreement. The results of both methods will be compared and the chemical bond in the title compound will be discussed on the basis of an MO model.

[1]: V.M.Padmanabhan, V.S.Yadava, Acta Cryst. B25,647(1969)

PS-16.01.11 A STUDY OF FERROELASTIC DOMAIN STRUCTURE WITH INCOMMENSURATE/COMMENSURATE TWIN BOUNDARIES BY MEANS OF AFM, STM, ESR, ESR-CT AND X-RAY DIFFRACTION. By T. Kobayashi^a and I. Takei, School of Pharmacy, Hokuriku University, Kanazawa, Japan and K. Yamana and S. Nakamura, Industrial Research Institute of Ishikawa, Kanazawa, Japan and M. Machida, Department of Physics, Faculty of Science, Kyushu University, Fukuoka, Japan.

The ferroelasticity of MP_5O_{14} ($M: \text{La-Tb}$) with commensurate domain boundaries and LaNbO_4 with incommensurate/ $\sqrt{2}$ ones (Sapriel, J. Phys. Rev., 1975, B12, 5128-) has been studied by DSC, polarizing microscope, X-ray diffraction, (Kobayashi, T. et al., J. Phys. Soc. Jpn., 1976, 40, 595-596), neutron diffraction (Horiuchi, H. et al., Jpn. J. Appl. Phys., 1991, 30, 2035-2039), ESR, ESR-CT, STM, and AFM. The domain structure near the boundary of $\text{GdP}_5\text{O}_{14}$ observed by AFM (nanoscope II) is shown in Fig.1. The large noises (obstacles) on the surface are removed by using the least squares method for the AFM scanning line as shown in Fig. 2. The XY projection of domain boundary AB on the crystal surface is shown in Fig. 3, the YZ projection in Fig. 4. The ferroelastic domain front seems to be a zigzag configuration in the microscopic observation. The domain wall width can be estimated from our AFM data. The temperature dependence of ferroelastic domain boundaries of $\text{EuP}_5\text{O}_{14}$ observed by STM is shown in Fig. 5. We observed the temperature dependence of monoclinic β angles, obtained by STM and X-ray diffraction (ω scan technique). According to Sapriel, LaNbO_4 should have incommensurate twin boundaries. The incommensurate twin boundaries, however, cannot be detected through our close analyses of neutron and X-ray diffractions by using the transformation matrix calculated from the UB matrix. Therefore if the incommensurate twin boundaries are supposed to exist, it is only close to the twin boundary wall. Our computer system of ESR crystallography will be also shown with the instruments (e.g. ESR 2/3-circle goniometer, ESR-CT etc.) developed specially for our experiments.

